Spatial Resolution of Gated X-ray Pinhole Cameras

H. F. Robey
K. S. Budil
B. A. Remington

MASTER

May 15, 1996

Lawrence Livermore National Laboratory

DISCLAIMER

Recycled
Recyclable

DISCLAIMER

Portions of this document may be illegible
in electronic image products.   Images are
produced from the best available original
document.

Spatial resolution of gated x-ray pinhole cameras

H.F. Robey, K.S. Budil, B.A. Remington
Lawrence Livermore National Laboratory, Livermore, CA 94550
(Presented on 15 May 1996)

We have conducted an investigation of the spatial resolution of a new gated x-ray pinhole camera, the FXI. The spatial resolution, or its Fourier transform the modulation transfer function (MTF), is critical for quantitative interpretation of recent hydrodynamic instability data taken on the Nova laser. We have taken data corresponding to backlit straight edges, pinholes, and grids, both on the bench and *in situ* on Nova. For both the pinhole and edge data, the MTF at all wavelengths of interest can be deduced from a single image. Grids are of more limited usefulness, giving the value of the MTF only at the spatial period of the grid. These different techniques for characterizing the MTF of gated x-ray pinhole cameras will be discussed, with results specific to the FXI presented.

I. INTRODUCTION

A series of experiments has been recently conducted on the Nova laser studying the Rayleigh-Taylor and Richtmyer-Meshkov instabilities of ablatively accelerated and shocked foils[1-3]. One of the most important diagnostics for these experiments is a new, flexible, gated x-ray pinhole camera (FXI)[4]. In order to quantitatively understand the dispersion relation (growth rate vs. wavenumber) of pre-imposed perturbations on such driven foils, one needs to fully understand the spatial resolution of the instrument. A degradation in the spatial resolution results in a loss of contrast in optical density, which if not properly taken into account would incorrectly be interpreted as a decrease in the perturbation growth. In this paper, we present the results of a series of experiments designed to measure the spatial resolution of the FXI over the full range of spatial scales of interest.

There are numerous possible sources of degradation of the instrument spatial resolution. In this paper, we focus on the two dominant sources, the finite spatial frequency response of the pinhole and the response of the microchannel plate (MCP). Figure 1 shows a schematic drawing of the MCP. The MCP used in the FXI has an active area of 40 mm diameter, thickness 0.5 mm, channel diameter 12 μm, channel pitch (pore-to-pore spacing) 15 μm, and bias angle of 8°. Electrons exiting the MCP are accelerated by a +4 kV accelerating voltage across a 0.5 mm gap to a phosphor screen. Some fraction of the photons created at the phosphor reflect off the back face of the MCP and create additional signal at the phosphor, leading to an observed glow about an otherwise sharp image[5]. In addition, a small fraction of the incident electrons will scatter elastically from the phosphor screen and will be redirected by the applied gap potential back toward the phosphor, again creating additional signal. These mechanisms form the dominant contribution which limits the instrument spatial resolution for spatial scales $\lambda \geq 30 \mu m$. For shorter scales, $\lambda < 20 \mu m$, the pinhole dominates.

2

II. IMAGE DATA

FXI images of several simple backlit targets which have been used to characterize the instrument spatial response are shown in Fig. 2. Images are shown both for data taken on a calibrated x-ray source and for *in-situ* data taken on Nova. Fig. 2(a) shows the results of a static bench measurement where a 5 mil Ta straight edge was mounted in close proximity to the MCP, and was illuminated with Al K-α x-rays generated by bombarding an Al anode with 5 keV electrons. There is a faint but distinct glow that extends under the Ta edge due to the finite spatial frequency response of the MCP. The corresponding edge data taken *in situ* on a Nova shot is shown in Fig. 2(b). Here a 1 mil straight edge of Au was back-illuminated with Sc He-α x-rays (hν=4.3keV), and imaged onto the MCP with 10 μm pinholes at 8x magnification. (Similar images have also been obtained at 12x.) The gate time was approximately 400 ps. This *in situ* measurement includes also the contribution to the resolution from the pinholes, but qualitatively looks very similar to the bench measurement. Figures 2(c) and 2(d) show similar images, but with the straight edge being replaced with a pinhole. In the bench measurement, the pinhole diameter was 300 μm, and in the Nova image the pinhole diameter is 40 μm. Finally, Figures 2(e) and 2(f) show *in situ* Nova data where Au grids were backlit with Sc x-rays. In Fig. 2(e), the grid wire period was 25 μm with 5 μm wide wires, whereas in Fig. 2(f), the wire period was 63 μm, and wire width was 15 μm. Both grid images were taken with the FXI at 12x magnification and 5 μm diameter pinholes.

III. ANALYSIS TECHNIQUE

Our spatial resolution analysis technique is illustrated in Fig. 3, with the *in-situ* straight-edge data. We start by creating an ideal image of a backlit straight edge, by masking off any light scattered under the edge as shown in Fig. 3(a). We then assume an azimuthally symmetric resolution function R(r), the Fourier transform of which is the modulation transfer function, or

MTF. The ideal edge image is then convolved with R(r), or in Fourier space, the 2D FFT of the ideal image is multiplied by the MTF. This results in the convolved edge image of Fig. 3(b). The convolution smears out the initial straight edge giving a glow underneath the edge which is similar in appearance to that observed in the original image of Fig. 2(b). We compare 1D lineouts taken across the convolved edge image with corresponding lineouts from the measured edge image of Fig 2(b), adjusting the parameters of the MTF or resolution function until the two agree. An example illustrating the result for the straight edge as measured on the bench is shown in Figures 4(a,b). As can be seen, the agreement between the two is excellent over the full spatial extent of the image. For the case shown, the MTF was found to be well fit by the following expression:

$$MTF(k) = \frac{1}{1.4}\left[e^{-(k/0.3927)^2} + 0.4e^{-k/0.0491}\right] \tag{1}$$

with the wavenumber magnitude $k = \sqrt{k_x^2 + k_y^2}$ given in radians/μm. A 1D lineout from the resulting resolution function R(r) is plotted in Fig. 5(a) for two magnifications, 8x and 12x. Fig. 5(b) shows a corresponding 1D lineout from the MTF. The MTF is shown for several Nova shots at 8x (solid curves, both edges and pinholes) and 12x (dashed curves, edge targets only). The MTF gives the *observed* contrast (variations in recorded ln(exposure)) that would be seen for an ideal (contrast=1) perturbation at each wavelength. At very short wavelengths, the instrument resolution is insufficient to resolve the contrast variation of the ripples, and the MTF approaches zero. At long wavelengths, the instrument spatial resolution is sufficient to completely resolve the ripples, and the MTF approaches one.

The data shown in Fig. 5(b) are all taken from Nova shots and therefore include the effects of both the MCP and the pinhole. In order to assess the relative contributions of each, we have calculated the effect of the pinhole separately. The long-dashed curve in Fig. 5(b) shows the MTF that would be obtained from the pinhole response alone with no contribution from the

4

MCP. This was calculated by computing the Fresnel near-field integral for a 10 μm pinhole at 8x magnification using a commercially available software package, ZEMAX[6]. We see that for λ ≥ 30 μm, the MCP is the dominant source of degraded resolution, while below this value both sources contribute to the instrument response. As indicated by the images in Fig. 2, we have used a variety of different techniques to characterize the FXI spatial resolution. All give results that agree with the MTF shown in Fig. 5(b) to better than 10%, as represented by the level of scatter in the cases which are plotted.

The backlit grids shown in Figs. 2(e,f) are of more limited usefulness. Grid images alone do not allow the tail of the resolution function to be quantified, but it is this tail that degrades the spatial resolution out to considerable spatial scales. Even if the functional form of the resolution function were known by independent means, the grid data could reliably produce values of the MTF only at modes corresponding to the fundamental period. To calculate the MTF from these grid images, 1D lineouts were Fourier transformed, and their magnitudes at the spatial period of the grid were compared with the corresponding values obtained from an ideal grid using a backlighter illumination pattern with the same spatial variation as in the original image. The result is shown by the two solid symbols in Fig. 5(b) corresponding to grid wire periods of 25 μm and 63 μm for the FXI at 12x magnification and 5 μm pinholes. Even though the 5 μm wide wires can be seen in the image shown in Fig. 2(e), the MTF at λ = 5 μm is approaching zero. The only reason we can see the wires is that the 5 μm thick Au wires have a very large contrast to the Sc backlighter x-rays, i.e., δ(OD) = 10. We can therefore see the wires, but only at a tiny fraction of the actual contrast.

IV. EFFECT OF MCP BIAS ANGLE ON AZIMUTHAL SYMMETRY

The non-zero bias angle of the MCP introduces a possible source of asymmetry to the response of the instrument. This effect has been extensively studied[5,7-9] in the literature. In [7], a

solution to Maxwell's equations was obtained for the electric field within the MCP channels, and it was shown that for very short times (<< 10 msec), the electric field is oriented perpendicular to the faces of the MCP. In this case, the output electrons acquire no transverse energy (parallel to the faces of the MCP), and there is no observed asymmetry due to the bias angle. For long exposures or DC operation, however, the electric field re-orients parallel to the channel walls, and in this case an asymmetry is observed. This effect has been observed in the pinhole measurements performed on the bench. An example is shown in Fig. 6, where images are shown for (a) a 10 sec exposure and (b) a 60 sec exposure of a 300 μm backlit pinhole. In (a), the scattering is essentially isotropic, whereas in (b) it is noticeably asymmetric with the scattering being skewed toward the top of the image. This direction is consistent with the orientation of the bias angle on the MCP, and is due to the transverse energy of the electrons exiting the MCP as studied extensively in [5]. Figure 7 shows lineouts taken from the images of Fig. 6 to quantify the asymmetry for these two exposure times. Figs. 7(a) and 7(b) show lineouts taken in the horizontal (x) and vertical (y) directions, respectively, for a 10 second exposure. In each case, the lineout is taken as an azimuthal average over $\pm 10°$ about the axis. In Figs. 7(a) and 7(b), the lineouts are symmetrical in both x and y. In Figs. 7(c) and 7(d), the same lineouts are plotted for the 60 sec exposure of Fig. 6(b). The scattering is still symmetrical horizontally, but in the vertical direction, there is a pronounced asymmetry with the magnitude of the scatter increased in the +y direction over the full spatial extent of the image. Under typical operation on Nova, however, this effect would not be observed as gate times are less than 1 nsec. It is only of importance for the present technique when one uses very long exposures in order to fully resolve the scattering tail of Fig 4(b). For such long exposures, the data can no longer be azimuthally averaged, but rather lineouts must be restricted to the horizontal axis, in which direction no effect of the bias angle is observed.

V. ACKNOWLEDGEMENT

REFERENCES

[1]M.M. Marinak *et al.*, Phys. Rev. Lett. **75**, 3677 (1995).

[2]K.S. Budil, Phys. Rev. Lett., in press (1996).

[3]T. Peyser *et al.*, Phys. Rev. Lett. **75**, 2332 (1995).

[4]K.S. Budil *et al.*, Rev. Sci. Instrum., **67**, 485 (1996).

[5]J.D. Wiedwald *et al.*, in *Ultrahigh- and High-Speed Photography, Videography, Photonics, and Velocimetry '90*, SPIE **1346** (1990).

[6]ZEMAX, Focus Software, Incorporated, Tuscon, AZ.

[7]E. Gatti *et. al.* , IEEE Trans. Nuclear Sci., **NS-30**(1) (1983).

[8]N. Koshida and M. Hosobuchi, Rev. Sci. Instrum. **56**(7), (1985).

[9]M. L. Edgar *et. al.*, Rev. Sci. Instrum. **60**(12), (1989).

FIGURE CAPTIONS

1) Schematic of the microchannel plate (MCP), illustrating the secondary scattering mechanisms

2) FXI backlit images of (a) straight edge on the bench, (b) straight edge on Nova, (c) 300 μm pinhole on the bench, (d) 40 μm pinhole on Nova, (e) 25 μm grid on Nova, and (f) 63 μm grid on Nova.

3) Illustration of the spatial resolution analysis technique. (a) "Ideal" backlit edge from Nova data. (b) "Ideal" Nova edge data convolved with FXI resolution function.

4) Comparison of the actual and convolved edge profiles for bench edge data of Fig. 2(a). (a) comparison of full edge profiles. (b) Expanded view of the tail.

5) (a) FXI resolution function for 8x and 12x magnifications. (b) FXI MTF vs. wavelength for several Nova shots at 8x and 12x. Solid points give MTF values obtained from the grid data at the wavelength corresponding to the grid periods of 25 and 63 μm. The theoretical MTF for a 10 μm pinhole only is shown for comparison.

6) The effect of MCP bias angle for long exposure times. 300 μm backlit pinhole bench measurement for (a) 10 sec and (b) 60 sec exposures.

7) Horizontal and vertical lineouts from pinhole data of Fig. 6 showing asymmetric scattering in the vertical direction as exposure time increases.
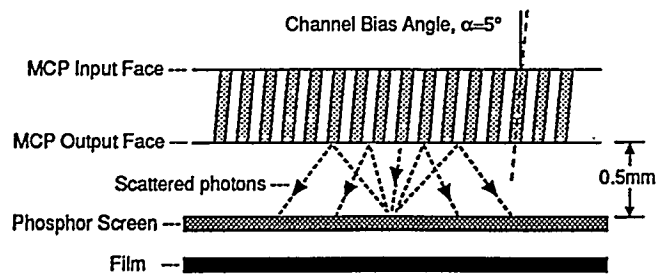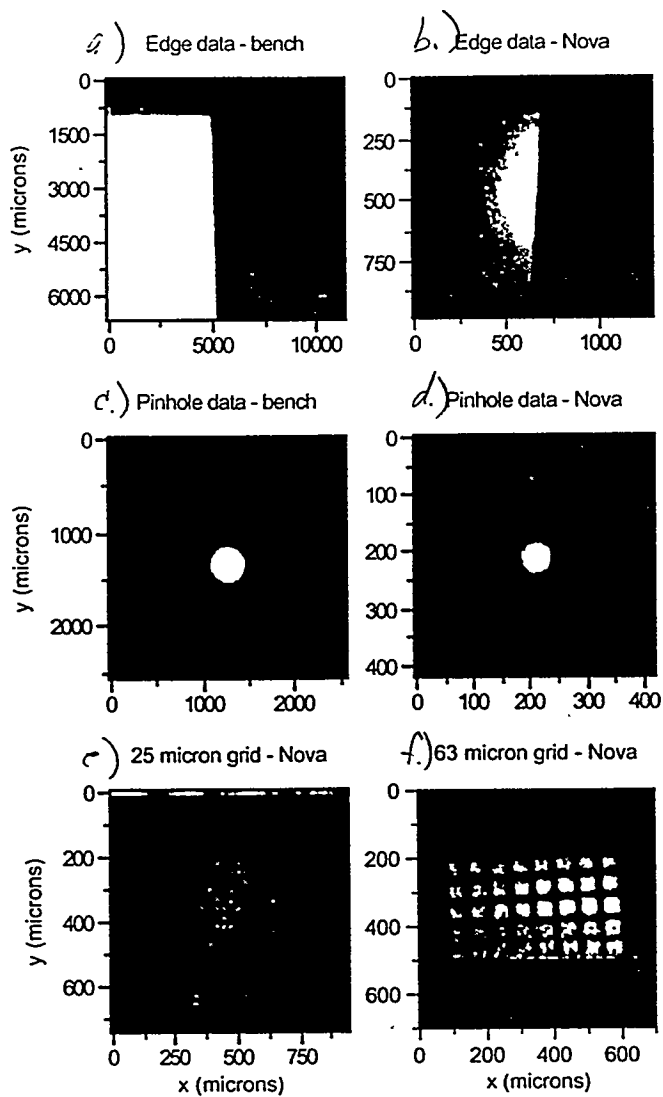
8

Channel Bias Angle, α=5°

MCP Input Face ---

MCP Output Face ---

Scattered photons ---

0.5mm

Phosphor Screen ---

Film ---

fig 1

a.) Edge data - bench   b.) Edge data - Nova

c.) Pinhole data - bench   d.) Pinhole data - Nova

e.) 25 micron grid - Nova   f.) 63 micron grid - Nova

fig 2
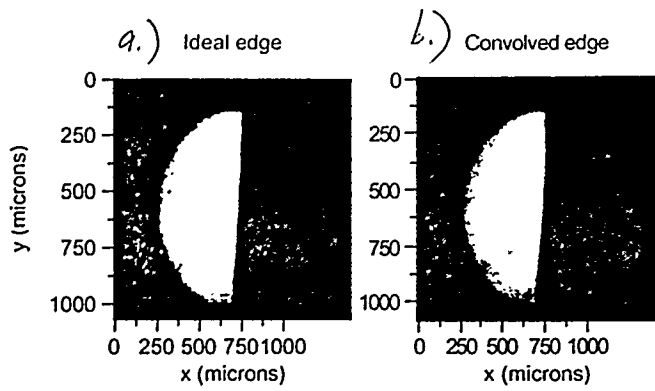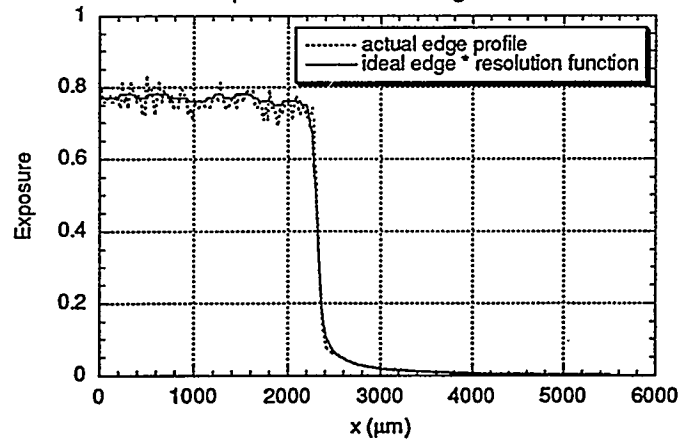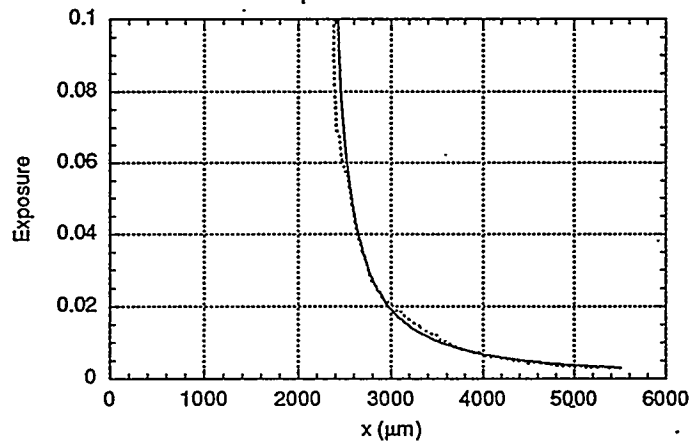
a.) Ideal edge   b.) Convolved edge

fig 3

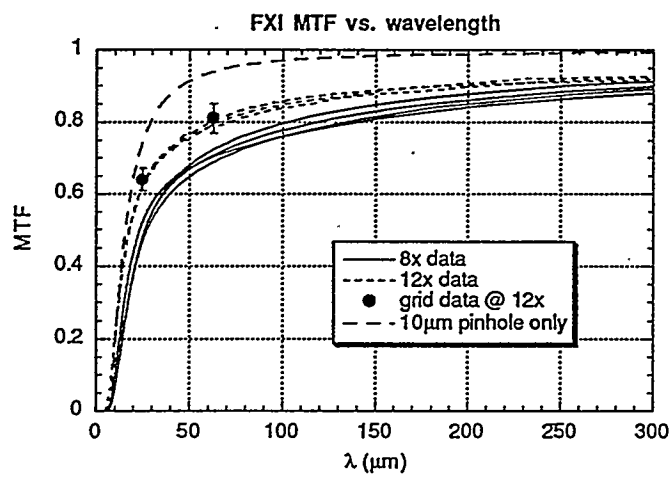FXI response to backlit edge - bench test
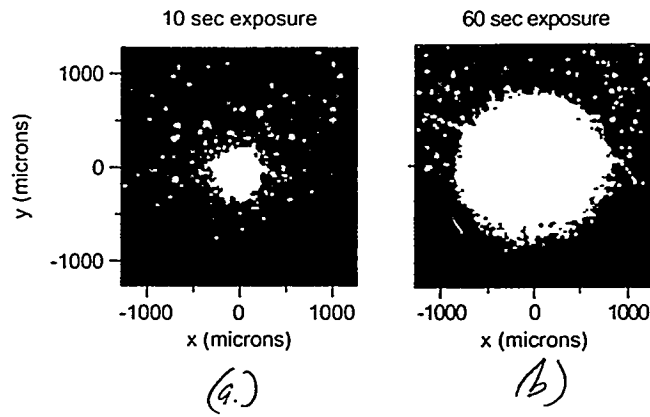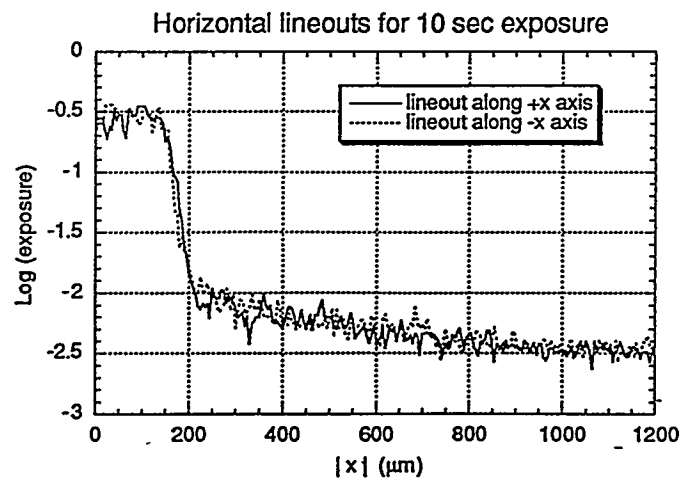

(a)

Expanded view of tail

(b)

fig 4.

Resolution function, R(r)

(a)

FXI MTF vs. wavelength

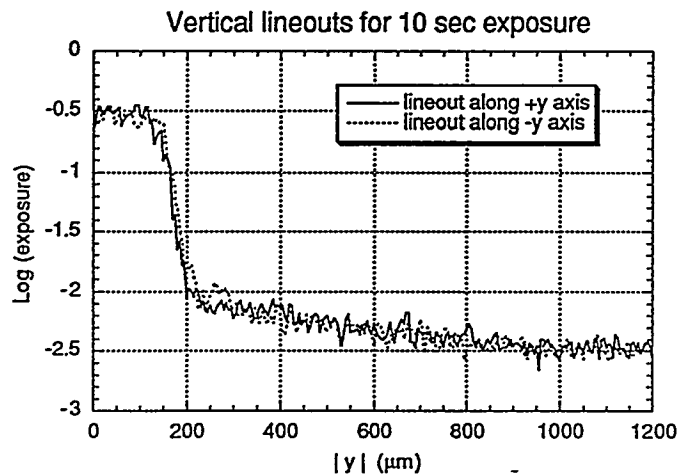(b)

fig 5

10 sec exposure   60 sec exposure

(a.)   (b)

fig 6

Horizontal lineouts for 10 sec exposure

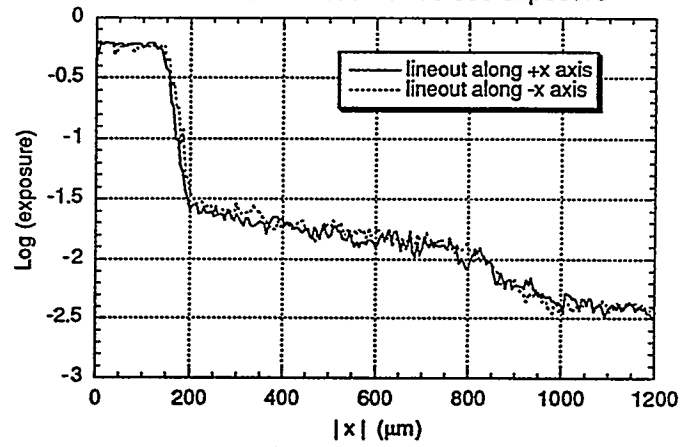(a)

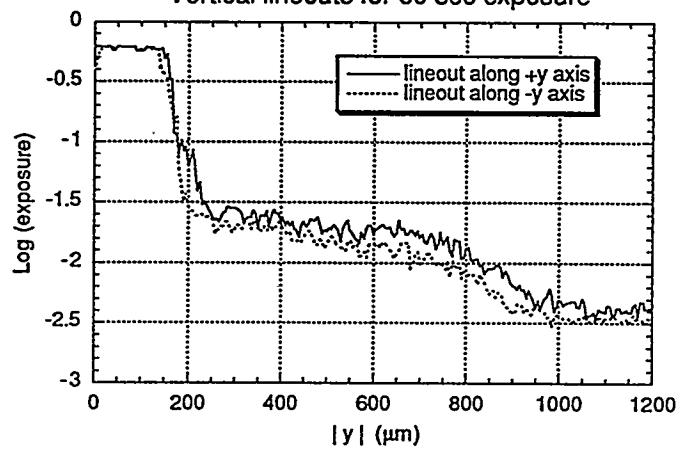Vertical lineouts for 10 sec exposure
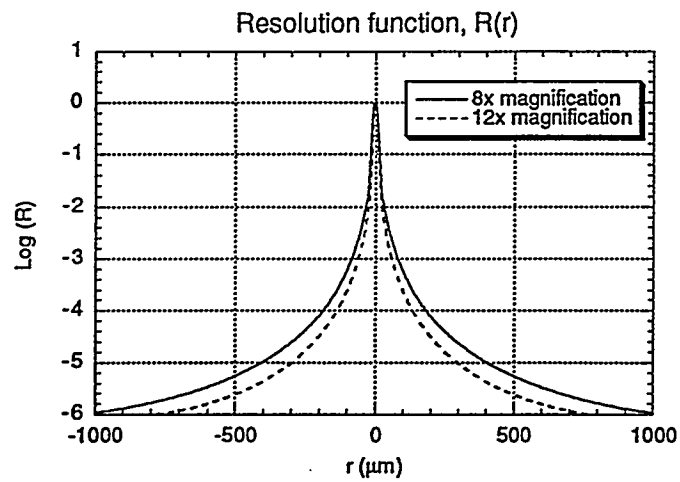
(b)

fig 7

Horizontal lineouts for 60 sec exposure

(c)

Vertical lineouts for 60 sec exposure

(d)

Fig 7